PNAS RESEARCH ARTICLE | MICROBIOLOGY

S-nitrosylation-triggered secretion of mycobacterial PknG leads to phosphorylation of SODD to prevent apoptosis of infected macrophages

Saradindu Saha[a,1], Sadhana Roy[a,1], Arnab Hazra[a], Debayan Das[a], Vimal Kumar[b], Amit Kumar Singh[b], Ajay Vir Singh[c], Rajesh Mondal[d,e], and Somdeb Bose Dasgupta[a,2]

Affiliations are included on p. 12.

Edited by Lalita Ramakrishnan, University of Cambridge, Cambridge, United Kingdom; received February 27, 2024; accepted January 24, 2025

The tuberculosis-causing agent *Mycobacterium tuberculosis* (M.tb) establishes its niche inside macrophages by secretion of several virulence factors and engaging many host factors. Mycobacterial infection of macrophages results in a proinflammatory trigger–mediated secretion of TNFα. Protein kinase G (PknG), a Serine/Threonine kinase, is essential for mycobacterial survival within the macrophage. Pathogenic mycobacteria, upon infection, can trigger the secretion of proinflammatory cytokine TNFα, but whether secreted PknG plays any role in TNFα secretion at early stages of infection remains undeciphered. Moreover, at early infection stages, prevention of macrophage apoptosis is vital to successful mycobacterial pathogenesis. Our studies show that mycobacteria-secreted PknG can dampen the expression and concomitant secretion of proinflammatory TNFα. During early infection, M.tb infection–induced generation of reactive nitrogen intermediates (RNI) leads to S-nitrosylation of PknG on Cys109, thereby enabling its secretion into macrophages. Upon M.tb infection, secreted S-nitrosylated PknG phosphorylates macrophage Silencer of Death Domains (SODD) at Thr405, as identified through our phosphoproteomic studies. Thereafter, phosphorylated SODD, through an irreversible binding with the TNFR1 death domain, prevents Caspase8 activation and concomitant extrinsic apoptotic trigger. Moreover, alveolar macrophages from mice infected with PknG-knockout M.tb also exhibited SODD phosphorylation and hindered Caspase8 activation to prevent extrinsic macrophage apoptosis. Therefore, this work exhibits S-nitrosylation-mediated secretion of PknG to induce phosphorylation of macrophage SODD, which, through irreversible interaction with TNFR1, prevented extrinsic macrophage apoptosis at the early stages of infection.

S-nitrosylation | protein kinase G | phosphorylation | SODD | apoptosis

Significance

Successful pathogens like mycobacteria can subvert macrophage proinflammatory responses and facilitate survival by secreting different virulence factors. This study exhibits how mycobacterial infection triggered proinflammatory response-generated RNI induces S-nitrosylation of mycobacterial PknG to facilitate its secretion into the macrophage cytosol. S-nitrosylated PknG dampens the expression and secretion of proinflammatory cytokine TNFα and phosphorylates macrophage SODD to enable its irreversible binding with TNFR1. This interaction prevents Caspase8-induced extrinsic apoptosis of mycobacteria-infected macrophages. "Dying to live" is an exit strategy inherent to macrophages, which is therefore successfully curtailed by pathogenic mycobacteria to establish its niche at the early stages of infection.

Tuberculosis (TB), caused by the *Mycobacterium tuberculosis* (M.tb), has plagued human civilization for ages (1). The prolonged treatment and patient noncompliance generate drug-resistant mycobacterial strains (2). An in-depth understanding of disease pathogenesis is essential to foster alternative therapeutic strategies. M.tb maintains a delicate balance between its intracellular proliferation and host damage during disease progression (3–5). According to the present paradigm, M.tb upon phagocytosis retards phagosome acidification and maturation to become acid tolerant such that it can later survive and proliferate inside phagolysosomes (6). To establish its niche inside macrophages, mycobacteria need to hinder macrophage apoptosis (7). Defense cells undergo apoptosis as part of their altruistic behavior (8) when they cannot defend against a pathogenic hijack (9). All pathogenic encounters initiate a proinflammatory response (10), which successful pathogens like mycobacteria (11) later alter to anti-inflammatory states. Critical triggers of proinflammatory response are the secretion of cytokines such as TNFα and IFNγ (12) and the generation of ROS and RNI (13). Through overexpression of SOCS1 and CISH, mycobacteria can dampen downstream signaling of IFNγ (14).

TNFα-induced programmed necrosis of macrophages is essential for mycobacterial dissemination and granuloma formation (15, 16). However, how mycobacteria tackle autocrine and paracrine TNFα signaling, which facilitate ROS and RNI formation and thereby boost macrophage apoptosis, remains to be elucidated. Binding of TNFα to TNFR1 can either promote cell survival through activation of NF-kB (17) or promote cell death with or without Caspase8 activation (18). Similarly, for M.tb infection, TNFα signaling is a double-edged sword (19) as it can either promote cell survival or cause cell death. The interplay of the interactors of TNFα bound TNFR1 determines the outcome, which for M.tb infection should be the promotion of host cell survival at the initial stage

The authors declare no competing interest.

This article is a PNAS Direct Submission.

[1]S.S. and S.R. contributed equally to this work.

[2]To whom correspondence may be addressed. Email: somdeb@iitkgp.ac.in.

This article contains supporting information online at https://www.pnas.org/lookup/suppl/doi:10.1073/pnas.2404106122/-/DCSupplemental.

Published March 4, 2025.

of infection to establish its niche and induce programmed necrosis at late stage of infection to facilitate mycobacterial dissemination. The TNFα signaling at early stages of infection remains elusive.

While viral proteins block the binding of TNFα with TNFR1 (20), pathogenic bacteria predominantly modify TNF-mediated responses (21) through secretion of virulence factors. A cross-talk between mycobacteria-secreted virulence factors and host proteins is critical to the subversion of the host immune system and the successful pathogenesis inside macrophages (22, 23). M.tb secretes several virulence factors, of which eukaryotic-like Serine/Threonine kinase: Protein kinase G (PknG) plays an essential role within macrophages (24). Inside mycobacteria, PknG regulates redox homeostasis (25) and glutamate metabolism (26), while inside macrophage cytosol, it hinders phagosome maturation (24)and thereby promotes mycobacterial pathogenesis. Why would the absence of PknG alone, in the presence of all other factors, trigger phagosome–lysosome fusion, more so because mycobacterial pathogenesis proceeds with acid tolerance and proliferation within phagolysosomes. PknG is capable of phosphorylating mycobacterial substrates and known to be secreted into macrophage cytosol upon infection. But surprisingly, till date, neither any phosphorylated macrophage substrate of PknG has been identified nor the role of these substrates in pathogenesis been elucidated.

TNFα signaling plays a critical proinflammatory role upon pathogen entry that initially facilitates lysosomal transfer of the pathogen, failing which apoptosis of infected macrophages would be triggered. Lacuna exists in the mechanism of dampened TNFα signaling at initial stages of mycobacterial infection, inhibition of macrophage altruism, and the absence of identified and characterized PknG-phosphorylated macrophage substrates. Hence, we hypothesized that mycobacteria-secreted PknG could modulate TNFα signaling to hinder macrophage apoptosis and thereby facilitate mycobacterial survival and proliferation. The binding of TNFα with TNFR1 results in receptor trimerization (27), causing the recruitment of TRADD (TNFR1-associated death domain protein) and FADD (Fas-associated death domain) (28) to form the death-inducing signaling complex (DISC), which then activates Caspase8. Reversible binding of Silencer of Death Domain (SODD) with the death domain of TNFR1(29) prevents constitutive DISC formation.

Here, we observe that infection with M.tb exhibits dampened expression and secretion of TNFα compared to PknG knockout M.tb. Comparative phosphoproteomics helped identify SODD as the phosphorylated macrophage substrates of PknG. We next elucidated how mycobacterial infection–induced proinflammatory trigger results in S-nitrosylation of PknG, to facilitate its secretion and concomitant phosphorylation of macrophage SODD. S-nitrosylated-PknG phosphorylated SODD binds irreversibly with TNFR1 to inhibit DISC formation, Caspase-8 activation, and thereby hinders macrophage apoptosis. M.tb-infected mice at early stages of infection also exhibit dampened TNFα expression and hindered alveolar macrophage apoptosis through secreted S-nitrosylated PknG-mediated SODD phosphorylation, while kinase-dead or S-nitrosylation inert PknG expressing M.tb mutant failed to prevent apoptosis of infected AVMΦ. This study elucidates the mechanism of S-nitrosylation of PknG and its concomitant secretion into macrophage cytosol to phosphorylate SODD and thereby prevent extrinsic macrophage apoptosis through inhibition of Caspase8 activation.

Results

Mycobacteria-Secreted PknG Causes Dampened TNFα Secretion and Hindered Caspase8 Activation. Mycobacteria survive within a delicate balance of pro and anti-inflammatory states (30). At late stages of infection, TNFα facilitates dissemination and granuloma formation (15). However, the same needs to be hindered at the initial stages of infection to enable M.tb survival and proliferation within macrophages.

It was observed that wild-type (Rv) mycobacteria-infected (6 h) THP-1 as compared to PknG knockout (RvΔPG) or PknG inhibitor AX20017 (AX17) pretreated THP-1 cells exhibited dampened TNFα secretion (Fig. 1*A*). Interestingly, THP-1 cells infected for 1 h with Rv exhibited a rise in secreted TNFα similar to RvΔPG-infected cells, but it was reduced at 6 h of infection (*SI Appendix*, Fig. S1*A*). The expression of TNFα was found to be dampened in Rv-infected THP-1 cells as compared to RvΔPG-infected or AX17 pretreated Rv-infected cells (Fig. 1*B*) which caused the dampened TNFα secretion from Rv-infected THP-1 cells.

Additionally, upon infection with RvΔPG, TNFα expression was dampened only in PG-expressing THP-1 cells. A luciferase assay using lysates from Rv-infected macrophages expressing the TNFα promoter construct exhibited similar results (Fig. 1*C*). Therefore, PG alone cannot dampen TNFα expression, but mycobacterial infection–generated milieu by facilitating the kinase activity of PG could induce dampened TNFα expression.

Since TNFα expression involves NFAT1 and ATF2 transcription factors, chromatin immunoprecipitation (ChIP) was next separately carried out using anti-NFAT1 and anti-ATF2 (*SI Appendix*, Fig. S1 *B* and *C*). Reduced levels of ATF2-binding sequence were obtained in the anti-ATF2 specific ChIP fractions of AX17 untreated, Rv-infected THP-1 cells or RvΔPG infected PG expressing THP-1 cells as compared to AX17 pretreated, Rv-infected, RvΔPG infected THP-1 cells alone or PG^{K181M} expressing THP-1 cells (Fig. 1*D*). While for the same cell types, equivalent levels of NFAT1 binding sequence were obtained (*SI Appendix*, Fig. S1*D*). Therefore, a reduced ATF2 binding to the TNFα promoter in Rv-infected cells, causing dampened TNFα expression and secretion, could emanate from structural alteration of ATF2 (possibly through PG-mediated phosphorylation) or reduced expression of ATF2 or rapid degradation of ATF2, all together or separately. Expression analysis of ATF2 did not exhibit any significant difference in the different infected and uninfected cells (*SI Appendix*, Fig. S1*E*). However, immunoblotting for ATF2 revealed a complete loss of ATF2 in Rv-infected THP-1 cells or RvΔPG-infected, PG-expressing THP-1 cells (Fig. 1*E*). This loss of ATF2 could be due to inhibition of ATF2 translation or rapid degradation of ATF2. A gradual loss of ATF2 was observed in the proteasomal inhibitor MG132 untreated cells, while MG132 pretreated cells exhibited multiple bands for ATF2, plausibly corresponding to its polyubiquitinated forms that were prevented from degradation (*SI Appendix*, Fig. S1*F*). Therefore, PG-induced rapid degradation of ATF2 results in reduced expression and secretion of TNFα in Rv-infected THP-1 cells. The mechanism of PG-induced rapid proteasomal degradation of ATF2 is a separate study, independent of the role of PG in the survival of Rv-infected macrophages.

Immunoblotting using anti-Caspase8 or assay using fluorogenic Caspase8 substrate exhibits cleaved Caspase8 or activated Caspase8 only for RvΔPG-infected THP-1 or PG^{K181M}-expressing THP-1 cells (Fig. 1*F* and *SI Appendix*, Fig. S1*G*). Caspase8 activation was prevented in RvΔPG-infected THP-1 cells incubated with anti-TNFα (*SI Appendix*, Fig. S1*H*), thereby indicating that secreted TNFα caused Caspase8 activation. Therefore, mycobacteria-secreted PG generates a milieu causing rapid degradation of ATF2 which dampens TNFα expression and secretion and thereby hinders Caspase8 activation.

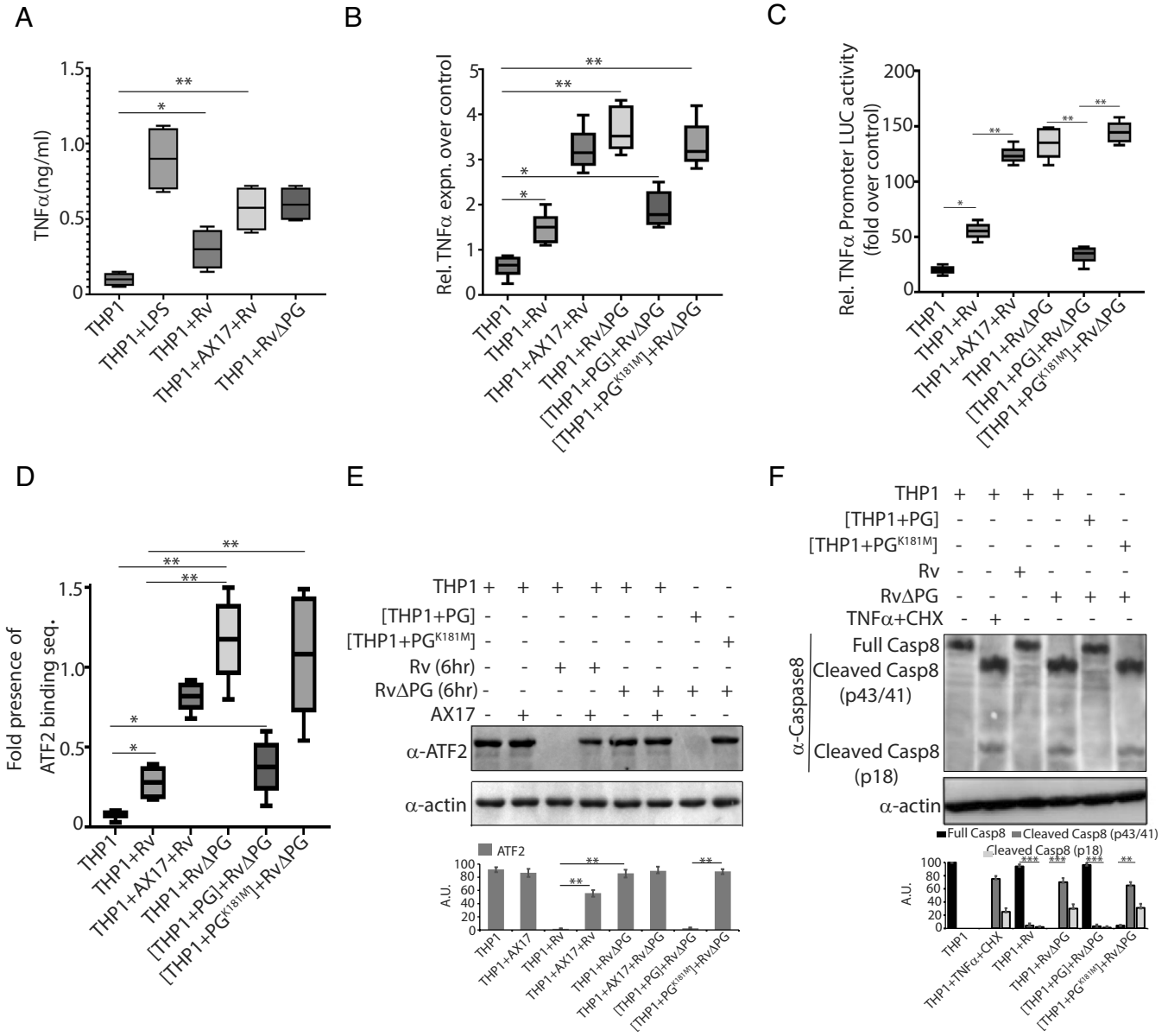

Fig. 1. Mycobacterial infection exhibits dampened TNFα secretion and hindered Caspase8 activation. (*A*) Secreted TNFα and (*B*) intracellular TNFα expression were measured by ELISA and qRT-PCR respectively from THP-1 cells (*A*) either uninfected, LPS treated, AX17 untreated or pretreated and Rv infected or RvΔPG only infected THP-1 cells and (*B*) uninfected, AX17 untreated or pretreated and Rv infected, RvΔPG only infected and PG/PG^{K181M} expressing THP-1 cells. The values in the graphs are mean ± SEM (n = 3). *$P < 0.05$ and **$P < 0.02$. (*C*) Luciferase assay for TNFα promoter activation from either untreated, AX17 untreated or pretreated and Rv or RvΔPG infected THP-1 cells as one set and either untransfected or PG/PG^{K181M} expressing, and RvΔPG infected THP-1 cells as another set. The values in the graphs are mean ± SEM (n = 3). (*D*) Fold presence of ATF2-binding, TNFα promoter sequence from ChIP fractions of uninfected, AX17 untreated or pretreated and Rv infected or RvΔPG infected THP-1 cells only or PG/PG^{K181M} expressing THP-1 cells. The values in the graphs are mean ± SEM (n = 3). *$P < 0.05$ and **$P < 0.02$. Immunoblotting of ATF2 from (*E*) uninfected, AX17 untreated or pretreated, and Rv or RvΔPG infected THP-1 or PG/PG^{K181M} expressing THP-1 infected with RvΔPG or from (*F*) THP-1 cells either uninfected or TNFα+CHX treated and Rv or RvΔPG infected for one set and THP-1 cells, either untransfected or expressing PG/PG^{K181M} and infected with RvΔPG for another set, were separately immunoblotted for Caspase-8 cleavage using an anti-panCas8 antibody. The values in the graph are mean ± SEM (n = 3).

Hindered Caspase8 Activation Is Due to Secreted S-Nitrosylated PknG-Mediated Phosphorylation of Macrophage SODD. The dampened TNFα secretion of Rv-infected THP-1 cells being three-fold higher than uninfected cells, should be activating Caspase8 and triggering apoptosis of infected macrophages, but the same is not evident. Separate PG-governed pathways are involved in hindering apoptosis of infected macrophages. Constitutive formation of the DISC complex facilitating Caspase8 activation is prevented by reversible binding of Silencer of the Death Domain (SODD) protein to the death domain of TNFR1 (18). Extracellular binding of TNFα to the TNFR1 alters its conformation to dislodge SODD and thereby enable TRADD-FADD binding and DISC formation to activate Caspase8 (31). Stabilizing the interaction of SODD with TNFR1, possibly through PG-mediated phosphorylation, could prevent Caspase8 activation. An in silico interaction studies of SODD, phospho-SODD (P-SODD), and TRADD with TNFR1 death domain exhibited that TNFR1 interacted the weakest with SODD and strongest with P-SODD (*SI Appendix*, Fig. S2 *A* and *B*), besides P-SODD exhibited altered binding residues and greater H-bonding with TNFR1 as compared to SODD. Therefore, M.tb infection–mediated secretion of PG and concomitant SODD phosphorylation could facilitate its irreversible binding with TNFα-bound TNFR1 and thereby prevent Caspase8 activation.

A comparative phosphoproteomic study (*SI Appendix*, Fig. S2*C*) was carried out. Volcano plots were generated using the ratio of

occurrence of phosphopeptides in the uninfected and Rv-infected THP-1 cells against the q-values obtained against these phosphopeptide ratios (*SI Appendix*, Fig. S2*D*, *Top*) and similarly using the ratio of occurrence of phosphopeptides in the AX17 pretreated alone, and AX17 pretreated and Rv-infected THP-1 cells against the respective q-values obtained against these phosphopeptide ratios (*SI Appendix*, Fig. S2*D*, *Bottom*). The phosphopeptides exclusively present in the *Top Right* corner of the *Bottom* (red box) of *SI Appendix*, Fig. S2*D* and absent in the *Top Right* corner were tabulated as the list of phosphorylated macrophage substrates of secreted PG. Using MASCOT, the protein identity for these phosphopeptides with high significance value and phosphorylation site were obtained (*SI Appendix*, Fig. S2*E*). Among these substrates, SODD had one of the highest q-values. Hence, we sought to validate SODD as a macrophage substrate of secreted PG and establish its role in hindering macrophage apoptosis both in vitro and in vivo.

An in vitro kinase assay was carried out using recombinant PG, PG^{K181M}, GarA, and SODD purified to essential homogeneity (*SI Appendix*, Fig. S2*F*). Bands corresponding to autophosphorylated PG and phosphorylated GarA alone (*SI Appendix*, Fig. S2*G*) were observed. Since PG is secreted inside macrophages only upon infection, we rationalized that infection-induced change in PG could facilitate its secretion and subsequent macrophage substrate phosphorylation; hence, PG-expressing THP-1 cells, upon infection with RvΔPG, exhibited dampened TNFα expression and secretion and hindered Caspase8 activation. All pathogens upon macrophage infection elicit a proinflammatory trigger which leads to the generation of ROS and RNI, which are destined to limit the infection, and the same is true after 1 h of Rv-infection of THP-1 cells where appreciable amount of TNFα is secreted. The four cysteine residues in the rubredoxin domain of PG form an (Fe-S) cluster (32), and cysteines of such clusters are prone to S-nitrosylation by RNI which thereby influence several signaling cascades (33).

Analysis of PG using GP-SNO database predicts a high S-nitrosylation score for Cys109 (*SI Appendix*, Fig. S3*A*). Therefore, a TMT-switch assay was carried out (*SI Appendix*, Fig. S3*B*) using RvΔPG-infected THP-1 cells expressing different cysteine mutants of PG as indicated (*SI Appendix*, Fig. S3*C*), where one part of the lysate was immunoprecipitated with anti-PknG and immunoblotted with anti-TMT while the rest of the lysates immunoblotted as indicated. For the anti-PknG immunoprecipitated fractions, the S-nitrosylated cysteines, now switched to iodoTMT, were detected using anti-TMT. Bands for TMT were observed in the wild-type PG and $PG^{C106,128,131G}$ mutants but not for the immunoprecipitated, $PG^{C106,109G}$ and $PG^{C106,109,128,131G}$ mutants for which the Cys109 was mutated. These results indicate that mycobacterial infection causes S-nitrosylation of PG at Cys109. Immunoblotting of the cell lysates exhibited phosphorylation of SODD only in those cells where Cys109 of PG is not mutated. Further, THP-1 cells expressing indicated PG mutants (*SI Appendix*, Fig. S3*D*) were infected with either RvΔPG or *M.smegmatis* (M.s) followed by immunoprecipitation with immunoblotting with anti-S-Nitrosocysteine antibody (34). Bands corresponding to S-nitrosylated PG were observed in all PG-expressing mutants except PG^{C109G}, both for RvΔPG- or M.s-infected cells, but SODD phosphorylation was observed only in PG- or PG^{C106G}-expressing cells infected with RvΔPG or M.s PG^{K181M}, although S-nitrosylated could not phosphorylate SODD as it was kinase dead. Besides, infection with either RvΔPG or M.s could create a milieu (plausibly by generating ROS and RNI) suitable for S-nitrosylation of PG at Cys109.

When the in vitro kinase assay using recombinant proteins was repeated (*SI Appendix*, Fig. S3*E*) in a GSNO (induces in situ S-nitrosylation of PG) containing buffer, bands of phosphorylated SODD were obtained in addition to autophosphorylated PG and phosphorylated GarA (*SI Appendix*, Fig. S3*F*). Our MS/MS study identified threonine 405 of SODD (S^{T405}) to be phosphorylated by PG. Hence, recombinant S^{T405A} mutant remained unphosphorylated in the kinase assay (*SI Appendix*, Fig. S3*G*). A similar kinase assay using cold ATP, followed by SDS-PAGE, transfer to PVDF membrane, and immunoblotting with anti-phospho Ser/Thr antibody, exhibits autophosphorylation of PG and phosphorylation of SODD only for PG and not for PG^{K181M}- or PG^{C109G}-expressing THP-1 (*SI Appendix*, Fig. S3*H*). Next, THP-1 cells without or with pretreatment with AX17, when infected with Rv or RvΔPG, when lysed, electrophoresed, transferred to PVDF, and immunoblotted with anti-P-SODD, exhibited bands in Rv-infected THP-1 cells while the same was dampened upon AX17 pretreatment (Fig. 2*A*). Similarly, when THP-1 cells expressing PG, PG^{K181M} or PG^{C109G} were infected with Rv or RvΔPG, bands for P-SODD was observed in all the Rv-infected cells (Fig. 2*B*) due to secretion of PG while for RvΔPG-infected, PG-expressing THP-1 cells, the infection generated milieu, facilitates the S-nitrosylation of transfected PG, which then phosphorylates SODD. When untreated or iNOS inhibitor, L-NMMA or RNI scavenger, 4DMAA pretreated THP-1 cells were infected with Rv or RvΔPG and immunoblotted with anti-P-SODD, bands were observed only for the Rv-infected cells, while the same were dampened considerably in L-NMMA and 4DMAA pretreated cells (Fig. 2*C*). Similarly, when THP-1 cells expressing either PG, PG^{K181M}, or PG^{C109G} were untreated or pretreated with AX17 or 4DMAA prior to infection with RvΔPG and thereafter lysed, immunoprecipitated with anti-PknG, and immunoblotted with anti-S-nitrosocysteine, bands corresponding to S-nitrosylated PG were observed in PG- or PG^{K181M}-expressing cells, and the same dampened in 4DMAA pretreated cells (Fig. 2*D*). Immunoblotting of the lysates exhibited bands for P-SODD only in the PG-expressing cells, and the same dampened in AX17 or 4DMAA pretreated cells. Therefore, it was evident that mycobacterial infection–generated RNI induces S-nitrosylation of PknG, which then phosphorylates macrophage SODD.

Mycobacterial Infection–Induced S-Nitrosylation of PknG Results in its Secretion and Concomitant SODD Phosphorylation. We next wanted to analyze whether PknG was S-nitrosylated inside the macrophage upon being secreted or was it S-nitrosylated inside mycobacteria upon infection and thereafter secreted into macrophage cytosol. In addition to Rv and RvΔPG, we generated complementing strains RvΔPG::PG, RvΔPG::PG^{K181M}, and RvΔPG::PG^{C109G}. All these mycobacterial strains exhibited similar growth kinetics (*SI Appendix*, Fig. S4*A*), were efficiently and equivalently phagocytosed by macrophages (*SI Appendix*, Fig. S4*B*), and had equivalent levels of cell wall lipid phthiocerol dimycocerosate (PDIM) (*SI Appendix*, Fig. S4*C*). Immunoblotting of these mycobacterial strains using anti-PknG exhibited equivalent PG, PG^{K181M}, or PG^{C109G} levels in the respective strains (*SI Appendix*, Fig. S4*D*). Mycobacterial chaperone SatS served as the control. Next, the wild-type and mutant complementing PknG knockout strains were treated with a NO donor, DEA-NONO in the presence of benzothiophene (BTP15), followed by lysis, immunoprecipitation using anti-PknG, and immunoblotting with anti-S-NitrosoCysteine. Bands corresponding to S-nitrosylated PknG were obtained from Rv or RvΔPG expressing PG and PG^{K181M} (*SI Appendix*, Fig. S4*E*). Secreted PG/PG^{K181M} measured through the ELISA was observed in supernatants of Rv, RvΔPG::PG, and PG^{K181M} (*SI Appendix*, Fig. S4*F*). Moreover, when THP-1 cells were infected with Rv,

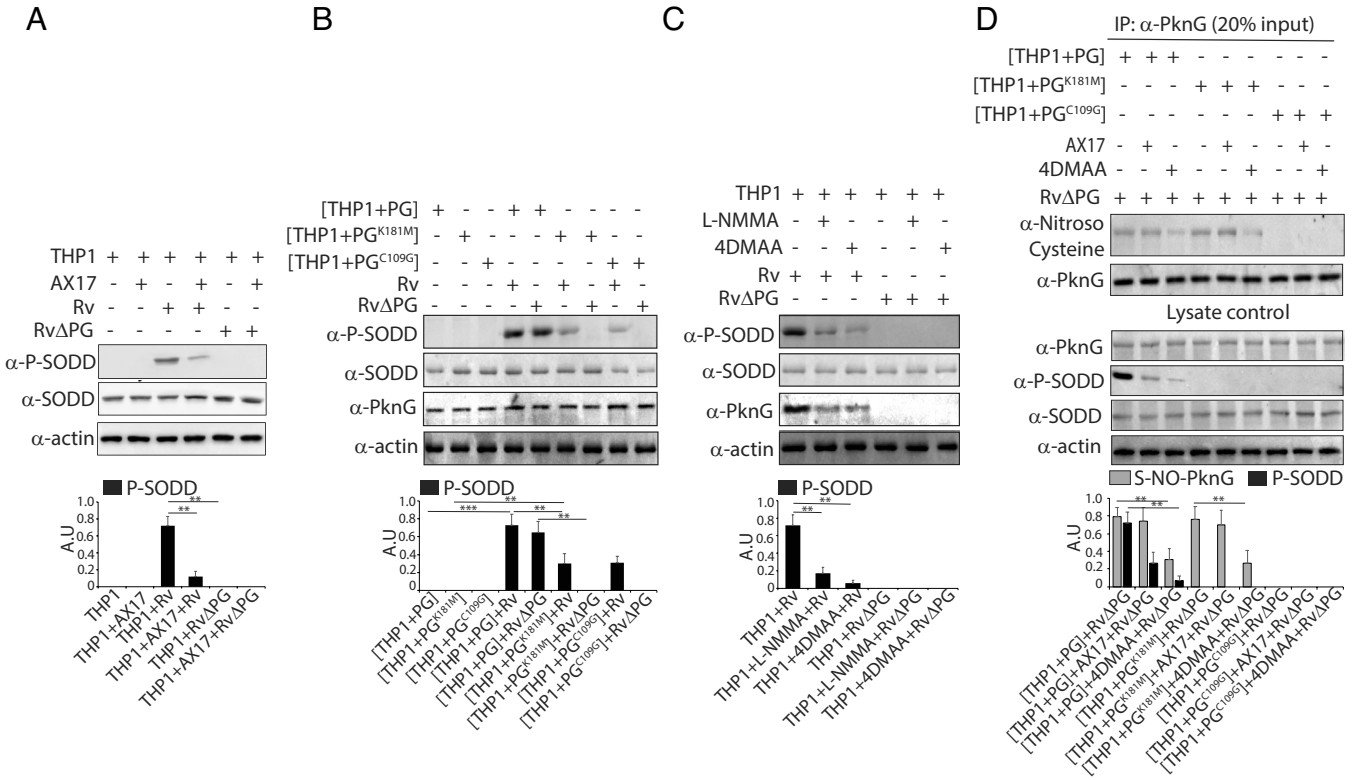

Fig. 2. Mycobacteria-secreted PknG can phosphorylate macrophage SODD at T405 only upon being S-nitrosylated (*A*) Rv- or RvΔPG-infected THP-1 cells which were either untreated or pretreated with AX17 or (*B*) PG-, PG^{K181M}-, or PG^{C109G}-expressing THP-1 cells infected with Rv or RvΔPG or (*C*) Rv- or RvΔPG-infected THP-1 cells which were either untreated or pretreated with L-NMMA and 4DMAA. (*D*) Immunoblotting for S-nitrosylated PG using anti-S-nitrosocysteine from anti-PknG immunoprecipitated fractions of RvΔPG-infected, PG/PG^{K181M}/PG^{C109G}-expressing THP-1 cells which were either untreated or pretreated with AX17 and 4DMAA. The lysates were immunoblotted for P-SODD.

RvΔPG::PG or RvΔPG::PG^{K181M} mycobacterial strains, PG was secreted by Rv or RvΔPG::PG and PG^{K181M} was secreted by RvΔPG::PG^{K181M} respectively inside macrophages but, SODD phosphorylation occurred only in Rv or RvΔPG::PG infected macrophages (Fig. 3*A*).

Furthermore, THP-1 cells expressing PG or its mutants, irrespective of infection, when treated with DEA-NONO, followed by lysis, immunoprecipitation with anti-PknG and immunoblotted with anti-S-nitrosocysteine exhibited bands corresponding to S-nitrosylated PG and PG^{K181M} in the respective protein- expressing THP-1 cells. P-SODD was present only in the S-nitrosylated PG-expressing THP-1 cells (Fig. 3*B*). THP-1 cells pretreated with L-NMMA or 4DMAA prior to infection with Rv or RvΔPG hindered the secretion of PG or PG^{K181M}, and only Rv-infected cells could secrete PG and thereafter phosphorylate SODD (Fig. 3*C*). Untreated or 4DMAA pretreated, THP-1 cells, alone or upon expressing indicated PG mutants were infected with RvΔPG, and thereafter lysed, immunoprecipitated with anti-PG, and immunoblotted using anti-S-nitrosocysteine. S-nitrosylated PG specific bands were observed only in PG and PG^{K181M} expressing cells, while the same were absent in mycobacteria infected, 4DMAA pretreated cells (*SI Appendix*, Fig. S4*G*). The lysates exhibited bands for P-SODD, only in the 4DMAA untreated, PG-expressing cells upon infection with RvΔPG. From these data, it is evident that infection-induced S-nitrosylation of PG inside the mycobacteria triggers its secretion into macrophage cytosol where it phosphorylates SODD, and irrespective of infection, treatment of PG-expressing macrophages with NO donor can also induce its S-nitrosylation, which then can phosphorylate SODD. Therefore, S-nitrosylation of PG emerges as an essential trigger for its secretion and macrophage substrate phosphorylation.

Appreciable CFU values corresponding to surviving M.tb inside macrophages were observed after 48 h of infection with Rv and RvΔPG::PG-infected mycobacteria (Fig. 3*D*). AX17 or 4DMAA pretreated cells, by inhibiting the kinase activity or S-nitrosylation of PG respectively, prevented SODD phosphorylation and therefore survival within macrophages. Furthermore, dampened TNFα secretion was observed from Rv- or RvΔPG::PG-infected macrophages, while RvΔPG alone or those expressing PG^{K181M}- or PG^{C109G}-infected macrophages exhibited appreciable levels of TNFα secretion (Fig. 3*E*). Similarly, RvΔPG alone or PG^{K181M}- or PG^{C109G}-expressing RvΔPG-infected cells exhibited Caspase8 cleavage (*SI Appendix*, Fig. S5*A*) and Caspase8 activation (*SI Appendix*, Fig. S5*B*) in comparison to Rv- or RvΔPG::PG-infected macrophages. Activated Caspase8 by cleaving BID generates t-BID to form pores on the mitochondrial outer membrane (MOMP) and thereby causes loss of mitochondrial membrane potential (MMP). Higher values of JC-1 fluorescence (580/530 nm ratio) indicative of normal MMP were observed only in Rv- and RvΔPG::PG-infected cells (*SI Appendix*, Fig. S5*C*), thereby indicating that infection with RvΔPG alone or when expressing PG^{K181M} or PG^{C109G} resulted in Caspase8 activation and concomitant loss of MMP. Downstream to the loss of MMP, executioner Caspase3 is activated, and the same was observed in cells infected with RvΔPG alone or when expressing PG^{K181M} or PG^{C109G} (*SI Appendix*, Fig. S5*D*). Staining with AnnexinV-PE (apoptosis-specific dye) and SYTOX Green (necrosis-specific dye) exhibited a high percentage of AnnexinV-PE-positive cells when infected with RvΔPG alone or when expressing PG^{K181M} or PG^{C109G} (*SI Appendix*, Fig. S5*E*, *Top*), while none of the cells exhibited SYTOX Green staining (*SI Appendix*, Fig. S5*F*, *Bottom*). SODD phosphorylation was absent in RvΔPG-, RvΔPG::PG^{K181M}-, or RvΔPG::PG^{C109G}-infected THP-1 cells. Lack of P-SODD

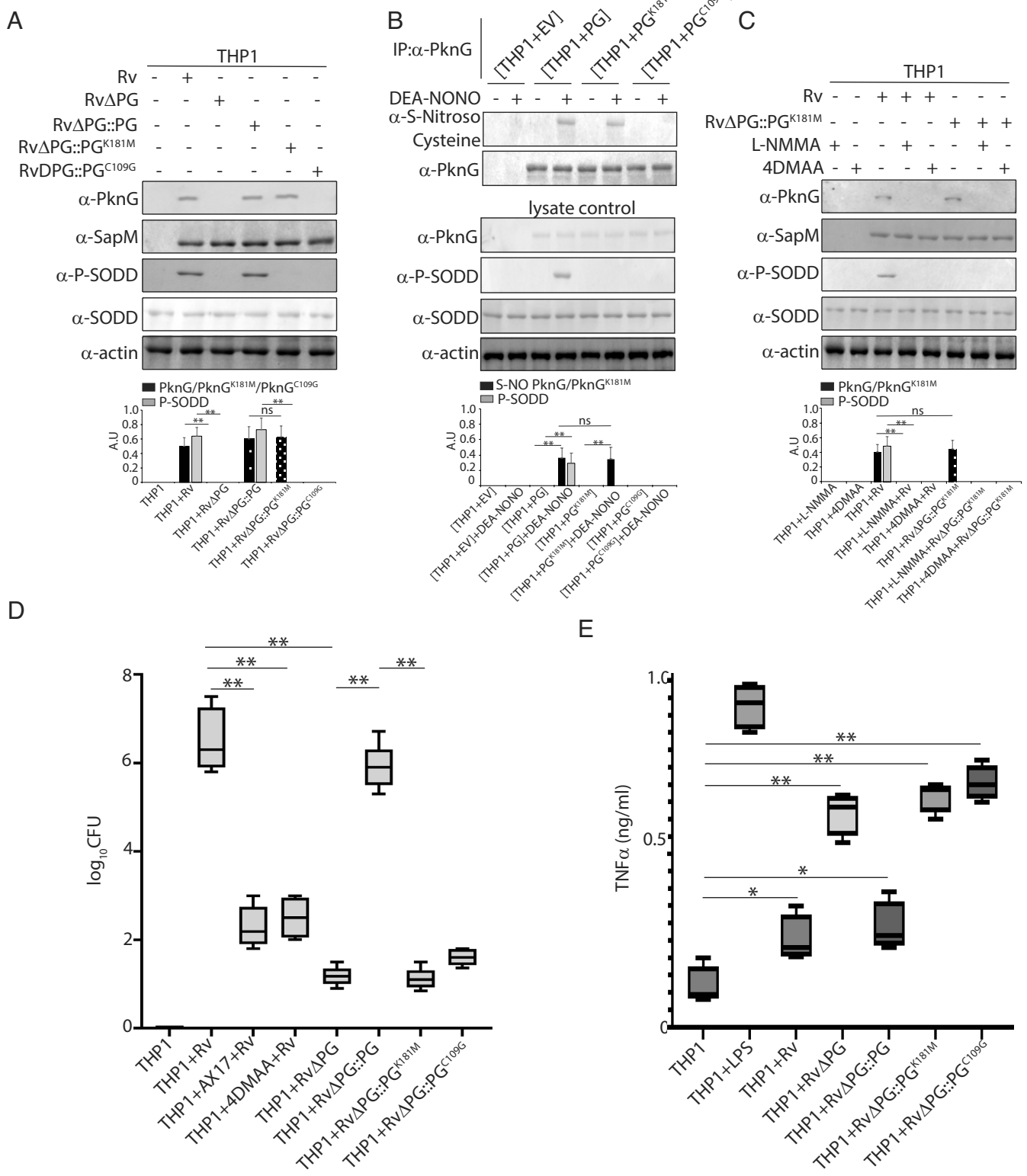

Fig. 3. Mycobacterial infection–generated RNI induces S-nitrosylation of PknG and its concomitant secretion. (*A*) Immunoblotting of THP-1 cells lysates after infection with, Rv, RvΔPG alone or RvΔPG expressing PG/PG^{K181M} or PG^{C109G}, using anti-PknG, anti-SapM and anti-SODD. The values in the graph are mean ± SEM (n = 3). (*B*) Immunoblotting of anti-PknG-immunoprecipitated fractions from DEA-NONO untreated or pretreated, lysates of THP-1 cells alone or expressing PG, PG^{K181M} or PG^{C109G}, with anti-PknG and anti-P-SODD. The values in the graph are mean ± SEM (n = 3). (*C*) Immunoblotting of untreated or L-NMMA or 4DMAA pretreated THP-1 cells upon infection with Rv or RvΔPG::PG^{K181M}, using anti-PknG, anti-SapM, and anti-P-SODD. The values in the graph are mean ± SEM (n = 3). (*D*) CFU assay of THP-1 cells alone or after AX17/4DMAA untreated or pretreated and Rv infection or upon infection with RvΔPG alone or expressing PG/PG^{K181M} or PG^{C109G}. All infections were done at MOI 10. The values in the graphs are mean ± SEM (n = 3). $^{**}P < 0.02$. (*E*) Extent of TNFα secretion measured by ELISA from supernatants of untreated, LPS treated, Rv, RvΔPG or PG/PG^{K181M}/PG^{C109G} expressing RvΔPG infected THP-1 cells. The values in the graphs are mean ± SEM (n = 3). $^{*}P < 0.05$ and $^{**}P < 0.02$.

results in the activation of Caspase8 and Caspase3, which then triggers apoptosis of the infected macrophages infected with these mycobacteria. A CFU assay using RvΔPG::PG-infected THP-1 cells exhibited appropriate CFU counts (*SI Appendix*, Fig. S5*G*). Apart from the uninfected THP-1 cells expressing different PG constructs, only RvΔPG::PG-infected cells did not exhibit Caspase8 activation (*SI Appendix*, Fig. S5*H*). Therefore, mycobacterial infection–induced S-nitrosylation of PG results in its secretion and concomitant SODD phosphorylation to prevent Caspase8 activation and apoptosis of infected macrophages.

Irreversible Binding of Phosphorylated SODD with TNFα Receptor Prevents Caspase8 Activation and Macrophage Apoptosis. To analyze the interaction of TNFR1 with P-SODD, AX17 or L-NMMA untreated or pretreated macrophages were infected with Rv and RvΔPG, lysed, immunoprecipitated with anti-SODD, and immunoblotted with anti-TNFR1 or anti-P-SODD. Bands corresponding to TNFR1 were observed for all the samples but were stronger only in Rv-infected cells, thereby exhibiting a more significant interaction (Fig. 4*A*). Bands for P-SODD were observed only in the Rv-infected cells, but the same decreased considerably in AX17 or L-NMMA pretreated cells. In a time course study of this interaction, macrophages were infected with Rv or RvΔPG, and thereafter lysed, immunoprecipitated with anti-TNFR1, and immunoblotted with indicated antibodies. Time dependent gradual increase in band intensity was observed which indicated an increasing interaction of P-SODD with TNFR1 in Rv-infected cells (Fig. 4*B*). In contrast, a gradually decreasing interaction of TNFR1 with TRADD was visible for the same time points. However, for increasing time of infection with RvΔPG, a gradually increasing interaction of TNFR1 with TRADD was observed. Taken together, it was evident that the interaction of SODD with TNFR1 is universal and reversible irrespective of Rv or RvΔPG infection, but with increasing time of infection with Rv, an increasing amount of P-SODD could compete with SODD and TRADD and bind irreversibly with the death domain of TNFR1, thereby preventing DISC formation and Caspase8 activation. With increasing time of infection with RvΔPG, reversibly bound SODD was dislodged, allowing TRADD to increasingly bind with TNFR1 and increasingly from DISC to activate Caspase8. Next, FLAG-TNFR1-DD$^{356–441}$ cloned under SOCS1 promoter (facilitates conditional expression inside macrophages, upon mycobacterial infection) and expressed in THP-1 cells when infected with Rv or RvΔPG exhibited equivalent expression of FLAG-TNFR1-DD$^{356–441}$ (anti-FLAG panel) and resultant Caspase8 activation and cleavage (*SI Appendix*, Fig. S6*A*). Of the differentially treated and infected macrophages, Caspase8 activation was prevented in Caspase8 inhibitor, Z-IETD-FMK pretreated, Rv or RvΔPG-infected cells. Hence, upon mycobacterial infection, S-nitrosylated PG-phosphorylated SODD competes with TRADD to bind irreversibly with TNFR1. However, mycobacterial infection–expressed FLAG-TNFR1-DD$^{356–441}$ by quenching P-SODD prevents its binding to endogenous TNFR1, thereby allowing TRADD binding to endogenous TNFR1 and concomitant DISC formation and Caspase8 activation even in Rv-infected cells. Further, fluorescence anisotropy measurements using recombinant and purified SODD$^{376–457}$, P-SODD$^{376–457}$, and TRADD$^{32–119}$ with TNFR1$^{356–441}$ death domain were carried out to obtain the dissociation constants (K_d) of the interaction (*SI Appendix*, Fig. S6*B*). Binding of P-SODD$^{376–457}$ with TNFR1-DD$^{356–441}$ exhibited the lowest K_d value while binding of SODD$^{376–457}$ with TNFR1-DD$^{356–441}$ had the highest K_d value, thereby indicating the strongest and weakest interactions, respectively.

Using CRISPR/Cas9, SODD knockout macrophages (S-KO) were generated (*SI Appendix*, Fig. S6*C*), and SODD (S-KO::S), phosphoinert SODD^{T405A} (S-KO::S^{A}), and phosphomimetic SODD^{T405E} (S-KO::S^{E}) were expressed in the S-KO cells (*SI Appendix*, Fig. S6*D*). Thereafter, wild-type, S-KO, and differentially complemented S-KO macrophages were infected with Rv

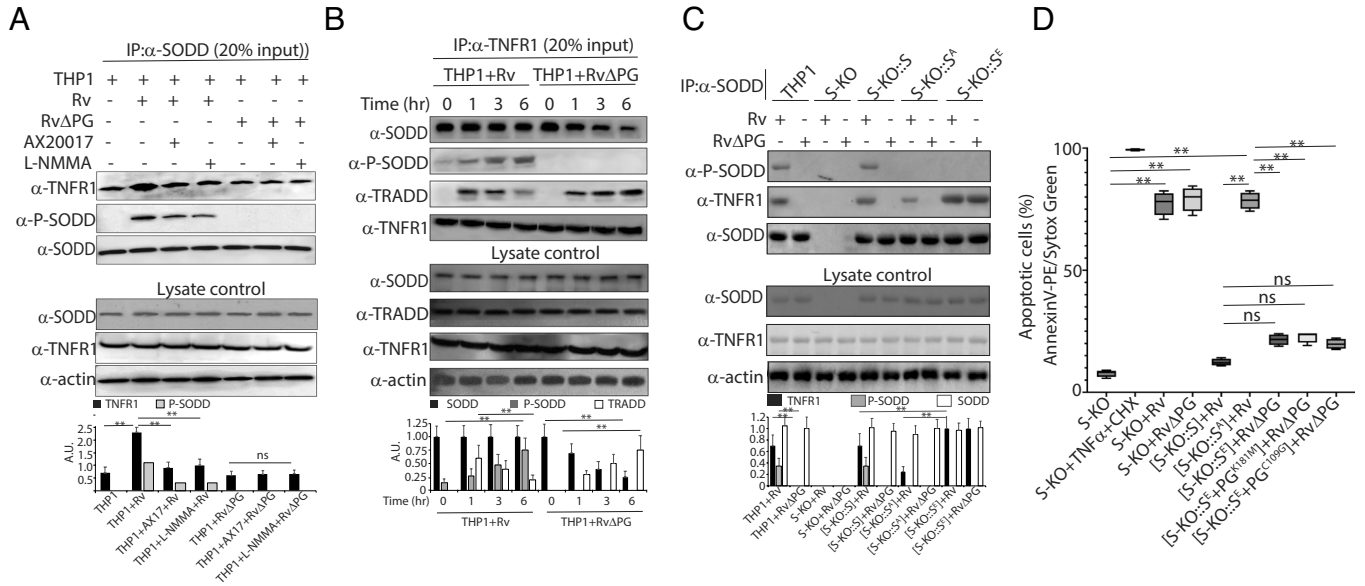

Fig. 4. Secreted S-nitrosylated PknG phosphorylates SODD to prevent Caspase-8 activation and concomitant macrophage apoptosis. (*A*) THP-1 cells, either untreated or pretreated with AX17 and L-NMMA and thereafter infected with Rv or RvΔPG, followed by lysis, immunoprecipitation with anti-SODD, and immunoblotting using indicated antibodies. The values in the graphs are mean ± SEM (n = 3). (*B*) THP-1 cells were infected with Rv or RvΔPG for indicated timepoints, followed by lysis, immunoprecipitation with anti-TNFR1, and immunoblotting with indicated antibodies. The values in the graphs are mean ± SEM (n = 3). (*C*) THP-1 and S-KO cells alone or expressing S, S^{A} or S^{E}, were infected with Rv or RvΔPG, followed by lysis, immunoprecipitation using anti-SODD, and thereafter immunoblotted as indicated. The values in the graph are mean ± SEM (n = 3). (*D*) Apoptosis was monitored in untreated or TNFα+CHX treated and Rv or RvΔPG infected S-KO cells as one set, Rv infected, S or SA expressing S-KO cells as second set and RvΔPG infected, only SE expressing or expressing PGK181M/PGC109G along with SE as third set upon AnnexinV-PE staining followed by Flow Cytometry. The values in the graph are mean ± SEM (n = 3). $^{**}P < 0.02$

and RvΔPG, lysed, immunoprecipitated with anti-SODD, and immunoblotted as indicated (Fig. 4*C*). Bands corresponding to P-SODD were observed in Rv-infected THP-1 and S-KO::S cells. In contrast, bands corresponding to TNFR1 were appreciably visible in Rv-infected THP-1, S-KO::S, and S-KO::S^E and negligibly in Rv-infected S-KO::S^A cells. Interestingly, bands for TNFR1 were also obtained in RvΔPG-infected S-KO::S^E cells as phosphomimetic S^E competes with TRADD similar to P-SODD without the requirement of PG secretion and SODD phosphorylation. Caspase8 cleavage assay was carried out in untreated or Caspase8 inhibitor Z-IETD-FMK pretreated S-KO and S-KO::S (*SI Appendix*, Fig. S6*E*) or S-KO::SA and S-KO::SE cells (*SI Appendix*, Fig. S6*F*) infected with Rv or RvΔPG. Bands corresponding to cleaved Caspase8 was observed in Rv and RvΔPG-infected S-KO cells, which were prevented upon Z-IETD pretreatment. However, S-KO::S cells exhibited Caspase8 cleavage only in RvΔPG-infected cells where secretion of S-nitrosylated PG and phosphorylation of complemented SODD do not occur (*SI Appendix*, Fig. S6*E*). For the complemented S^A-expressing cells, infection with both Rv and RvΔPG resulted in Caspase8 activation and cleavage, and it was prevented in Z-IETD-pretreated cells since even upon Rv infection, secreted S-nitrosylated PG could not phosphorylate complemented S^A in the S-KO cells (*SI Appendix*, Fig. S6*F*, lanes 1–5). Interestingly, Caspase8 activation and cleavage were hindered both in Rv- and RvΔPG-infected S-KO::S^E cells as the presence of phosphomimetic S^E, irrespective of the presence of secreted S-nitrosylated PG upon Rv infection or its absence in RvΔPG-infected cells, could interact with TNFR1 and thereby prevent Caspase8 activation and cleavage (*SI Appendix*, Fig. S6*F*, lanes 6–10). Furthermore, a fluorogenic substrate-cleavage-based Caspase8 activation assay revealed similar results where infection of S-KO with Rv resulted in Caspase8 activation. Complementation of S-KO with S hindered Caspase8 activation upon infection with Rv alone (*SI Appendix*, Fig. S7*A*). Expression of PG but not PG^{K181M} or PG^{C109G} along with S in S-KO hindered Caspase8 activation upon RvΔPG infection. However, complementation with S^A alone or with PG, irrespective of infection with Rv or RvΔPG, exhibited Caspase8 activation because S^A could not bind to TNFR1. On the contrary, complementation with S^E alone or with PG or PG^{K181M} or PG^{C109G}, irrespective of infection with Rv or RvΔPG, failed to activate Caspase8 owing to irreversible binding of S^E with TNFR1. Moreover, the Caspase3 activation assay exhibited results similar to that observed for Caspase8 activation (*SI Appendix*, Fig. S7*B*), thereby indicating that Caspase3 activation, as usual, occurred downstream to Caspase8 activation.

We next measured TNFα secretion from S-KO cells alone or complemented with S or its mutants and expressing PG or its mutants upon infection with Rv or RvΔPG alone or complemented with PG as has been indicated (*SI Appendix*, Fig. S7*C*). It was observed that dampened TNFα secretion occurred for all cell types where wild-type PG is present, i.e., upon being secreted by Rv or RvΔPG::PG or on the expression of PG inside macrophages. TNFα secretion was not dependent on S, as S, S^A, and S^E complemented strains alone, upon infection with RvΔPG, exhibited increased TNFα secretion similar to RvΔPG-infected THP-1 cells, as was observed earlier. Therefore, it can be concluded that dampened TNFα secretion and S-nitrosylated PknG-mediated phosphorylation of SODD to hinder Caspase8 activation are two distinct events separately regulated by S-nitrosylated PknG upon being secreted into macrophages. Rv- and RvΔPG-infected S-KO cells exhibited apoptosis owing to the absence of S and PG along with S, respectively (Fig. 4*D*). Complementation of S-KO with S and not S^A could only prevent macrophage apoptosis upon Rv infection. In contrast, complementation with S^E alone or with PG^{K181M} or PG^{C109G} in S-KO cells upon infection with RvΔPG did not exhibit apoptotic death. These observations indicate that mycobacterial infection induced S-nitrosylation of PG, resulting in SODD phosphorylation could hinder macrophage apoptosis. We carried out a CFU assay to further observe the effect of P-SODD/S^E hindered Caspase8 activation on mycobacterial survival within macrophages (*SI Appendix*, Fig. S7*D*). Appreciable CFU was observed in S-complemented S-KO cells upon infection with Rv due to the presence of secreted S-nitrosylated PknG, which phosphorylates complementing S, and also in S^E-complemented S-KO cells upon infection with RvΔPG as S^E mimics P-SODD and interacts with TNFR1 to hinder Caspase8 activation and macrophage apoptosis. Complementation with S^A followed by Rv infection failed to exhibit appreciable CFU as these cells undergo Caspase8-triggered apoptosis. Additionally, Rv-infected S-KO::S^A cells, although having secreted S-nitrosylated PG capable of hindering phagosome-lysosome fusion, were unable to promote macrophage survival owing to activation of Caspase8-triggered apoptosis of the infected macrophages. These data suggest that prevention of macrophage apoptosis is crucial to mycobacterial survival and proliferation with the macrophage.

Secreted S-Nitrosylated PknG-Phosphorylated SODD Prevents Apoptotic Death of Mycobacteria-Infected Mice Alveolar Macrophages. The in vitro observed results validated in vivo in BALB/c mice infected separately using aerosolized Rv, RvΔPG, RvΔPG::PG, RvΔPG::PG^{K181M} and RvΔPG::PG^{C109G} (*SI Appendix*, Fig. S8*A*). Immunofluorescence, as well as immunoblot analysis of alveolar macrophages(AVMϕ) isolated from bronchoalveolar lavage (BAL) of these mice, after 48 h of infection, exhibited SODD phosphorylation in Rv- and RvΔPG::PG-infected cells where no cleaved Caspase8 was observed (Fig. 5 *A* and *C*). However, for RvΔPG alone or PG^{K181M}- and PG^{C109G}-expressing mycobacteria-infected mice AVMϕ, P-SODD was absent, and instead, cleaved Caspase8 was visible [Fig. 5 *A* and *B* (*Top*) and (*Bottom*)]. Additionally, immunoprecipitation of these isolated AVMϕ with anti-PG followed by immunoblotting with S-nitrosocysteine exhibited bands corresponding to S-nitrosylated PG in Rv-, RvΔPG::PG-, and RvΔPG::PG^{K181M}-infected mice isolated AVMϕ fractions (Fig. 5*C*).

Furthermore, analysis for activated Caspase8 from lysates of the same isolated AVMϕ exhibited positive values for RvΔPG alone or PG^{K181M}- and PG^{C109G}-expressing mycobacteria-infected mice AVMϕ (*SI Appendix*, Fig. S8*B*). Concomitant to Caspase8 activation when loss of MMP was monitored using JC-1 dye, significantly high values were obtained for uninfected, Rv and RvΔPG::PG-infected mice isolated AVMϕ fractions (*SI Appendix*, Fig. S8*C*). Therefore, it can be inferred that there was no loss of MMP in these isolated AVMϕ, while for the knockout or PG mutant expressing AVMϕ, there was a loss of MMP. Consequent to the loss of MMP, MOMP can be formed, which can be monitored by observing the cytoplasmic release of mitochondrial cytochrome C (CytC). Immunoblotting for CytC, exhibited bands in AVMϕ (isolated from BAL of infected BALB/c mice) lysates upon infection with RvΔPG alone or RvΔPG expressing PG^{K181M}/PG^{C109G}. (*SI Appendix*, Fig. S8*D*). Thus it was evident that MOMP was formed in these macrophages, consequent to Caspase8 activation and loss of MMP. Formation of MOMP is known to activate the executioner caspase; Caspase3. Hence, RvΔPG alone or PG^{K181M}/PG^{C109G}-expressing RvΔPG infected mice obtained AVMϕ, exhibited Caspase3 activation (*SI Appendix*, Fig. S8*E*). Consequent to Caspase3 activation, nuclear DNA

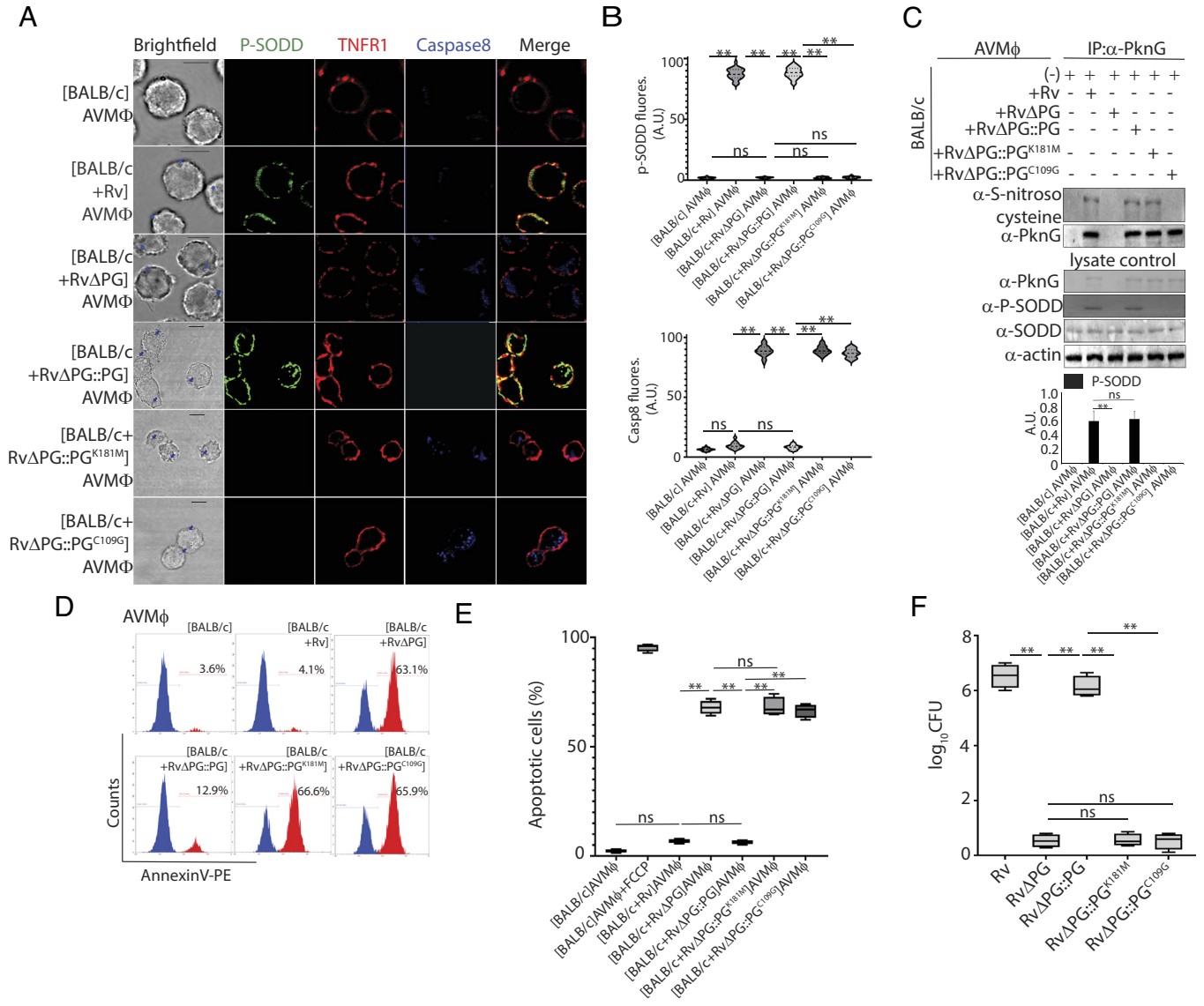

Fig. 5. M.tb-infected mice exhibit secreted S-nitrosylated PknG-mediated SODD phosphorylation to hinder Caspase8 activation and thereby inhibit macrophage apoptosis. (*A*) Immunofluorescence analysis of AVMΦ (isolated from BAL of BALB/c mice) either uninfected or infected for 48 h with Rv, RvΔPG alone or RvΔPG expressing PG/PG^{K181M} or PG^{C109G}, using anti-P-SODD (green-AlexaFluor488), anti-TNFR1 (red-AlexaFluor568) and anti-Casp8 (blue- AlexaFluor647) as indicated. Blue arrows in brightfield indicate infected mycobacteria. (Scale bar 10 μm.) (*B*) SODD phosphorylation (*Top*) and (*Bottom*) Caspase8 activation in AVMΦ isolated from BAL of uninfected or Rv/ RvΔPG/RvΔPG::PG/ RvΔPG::PG^{K181M} or RvΔPG::PG^{C109G}-infected BALB/c mice. The values in the violin plot are mean ± SEM (n = 50). $^{**}P < 0.02$ (C) Immunoblotting of anti-PknG immunoprecipitated fractions of AVMΦ isolated from BAL of BALB/c mice infected with Rv or RvΔPG alone or upon expressing PG/PG^{K181M} or PG^{C109G}, using anti-S-nitrosocysteine, while lysates of same cells immunoblotted with anti-PknG and anti-P-SODD. The values in the graph are mean ± SEM (n = 3). Flow cytometric analysis of apoptotic induction in AnnexinV-PE stained AVMΦs, isolated from BAL of Rv, RvΔPG alone or RvΔPG expressing PG/PG^{K181M} or PG^{C109G}, infected BALB/c mice, data represented as (*D*) histogram or (*E*) box plot. The values in the box plot are mean ± SEM (n = 3). $^{**}P < 0.02$. (*F*) CFU analysis of Rv, RvΔPG or PG/PG^{K181M} or PG^{C109G} expressing RvΔPG infected BALB/c mice. All infections were done at MOI 10, and infection proceeded for 21 d, followed by plating of isolated lung homogenates. The values in the graphs are mean ± SEM (n = 3). $^{**}P < 0.02$.

fragmentation is initiated. Therefore, when TUNEL assay was carried out, dUTP-FITC-positive nuclei were observed from RvΔPG alone or PG^{K181M}/PG^{C109G} expressing RvΔPG, infected mice-obtained AVMϕ (*SI Appendix*, Fig. S8*F* (*Top* and *Bottom*) and *H*). Hence, it was evident that mycobacteria-secreted S-nitrosylated PG in Rv- or RvΔPG::PG-infected mice prevents apoptosis of the infected AVMϕs.

Further, when we analyzed the extent of apoptosis through AnnexinV-PE and SYTOX-Green staining of these isolated AVMϕs, it was observed that mycobacteria-secreted S-nitrosylated PG in Rv- or RvΔPG::PG-infected mice prevents apoptosis of the infected AVMΦs. While RvΔPG alone or PG^{K181M}/PG^{C109G} expressing RvΔPG, infected mice-obtained AVMϕ, exhibited positive AnnexinV-PE staining, Rv or RvΔPG::PG infected mice obtained AVMϕ exhibited minimal AnnexinV-PE positive cells (Fig. 5 *D* and *E*) thereby indicating induction of apoptosis in the wildtype PG negative cells. None of the isolated AVMϕs exhibited appreciable SYTOX Green staining, indicating no necrotic cell death induction (*SI Appendix*, Fig. S8*G*). Finally, the CFU assay was carried out, at 21 d postinfection, to monitor the mycobacterial load upon infection of mice with equal amounts of aerosolized mycobacterial strains. Positive CFU counts were only observed for Rv- and RvΔPG::PG-infected mice 21 d postinfection (Fig. 5*F*), indicating that these mycobacteria could survive and proliferate inside alveolar macrophages. In contrast, RvΔPG, RvΔPG::PG^{K181M}, and RvΔPG::PG^{C109G} failed to survive either due to apoptosis of the infected AVMΦ or rapid transfer to the lysosome and therefore exhibited a low CFU count. Taken together it can be concluded that, M.tb infection induced S-nitrosylation of mycobacteria resident PG, results in its secretion and

concomitant SODD phosphorylation. Thereafter P-SODD by binding irreversibly with TNFR1, prevents Caspase8 activation and thereby hinders macrophage apoptosis to facilitate mycobacterial survival and proliferation both in vitro and in vivo. (Fig. 6)

Discussion

Secretion of virulence factors is among the plethora of mechanisms through which M.tb can subvert macrophage defense strategies. PknG is a secreted kinase whose role in mycobacterial pathogenesis to date has been attributed to functions other than phosphorylation of macrophage substrates. PknG harbors TPR and rubredoxin domains, which can interact with proteins irrespective of phosphorylation (35). Compared to PknG-knockout, wild-type M.tb-infected macrophages exhibit a significantly dampened TNFα expression and secretion owing to PknG-induced rapid degradation of the TNFα promoter-specific transcription factor, ATF2. Wild-type M.tb-infected macrophages, by exhibiting dampened TNFα secretion, prevented auto- or paracrine signaling-mediated Caspase8 activation. Hence, we hypothesized that PknG could be curbing macrophage altruism early during infection through phosphorylation of macrophage substrates.

PknG is known not to be secreted constitutively, but inside mycobacteria, PknG is capable of phosphorylating GarA and ribosomal L13 (26, 36). Surprisingly, our comparative phosphoproteomic screen although identified macrophage SODD as a substrate of PknG, recombinant PknG in our initial in vitro kinase assay failed to phosphorylate SODD. Like to all pathogens, M.tb infection, at its onset, exhibits a proinflammatory response through the formation of ROS and RNI, but mycobacteria can successfully dampen these responses. The rubredoxin domain of PknG, through its four cysteine residues, forms a (Fe-S) cluster (32), and cysteine of such (Fe-S) clusters is prone to S-nitrosylation, which inside mycobacteria could be triggered by infection-generated host RNI or a ROS/RNI-activated mycobacterial S-nitrosylase. Therefore, S-nitrosylation of PknG may enable it to leave behind its intramycobacterial metabolic role and acquire the required secretory impetus to cross the mycobacterial and phagosome barriers and get secreted into macrophage cytosol and thereby phosphorylate macrophage substrates to facilitate mycobacterial pathogenesis.

S-nitrosylation has been reported to activate other secreted bacterial kinases, thereby influencing their host–pathogen interaction (37). We observed that PknG was S-nitrosylated on cysteine 109 upon infection through bioinformatic and biochemical experiments. Upon addition of GSNO (adds NO to cysteines in vitro) to the in vitro kinase buffer, recombinant PknG could phosphorylate SODD. Therefore mycobacterial infection triggered proinflammatory milieu through activation of iNOS, resulting in RNI formation. These generated RNI (NO*, ONOO*) upon entering phagosome resident mycobacteria could directly or indirectly induce S-nitrosylation of PknG. Hence, S-nitrosylation of PknG and concomitant SODD phosphorylation was hampered in iNOS inhibitor and RNI scavenger pretreated cells, upon infection with Rv. Additionally, a NO donor, DEA-NONO-treated mycobacteria exhibited S-nitrosylation of PknG irrespective of infection.

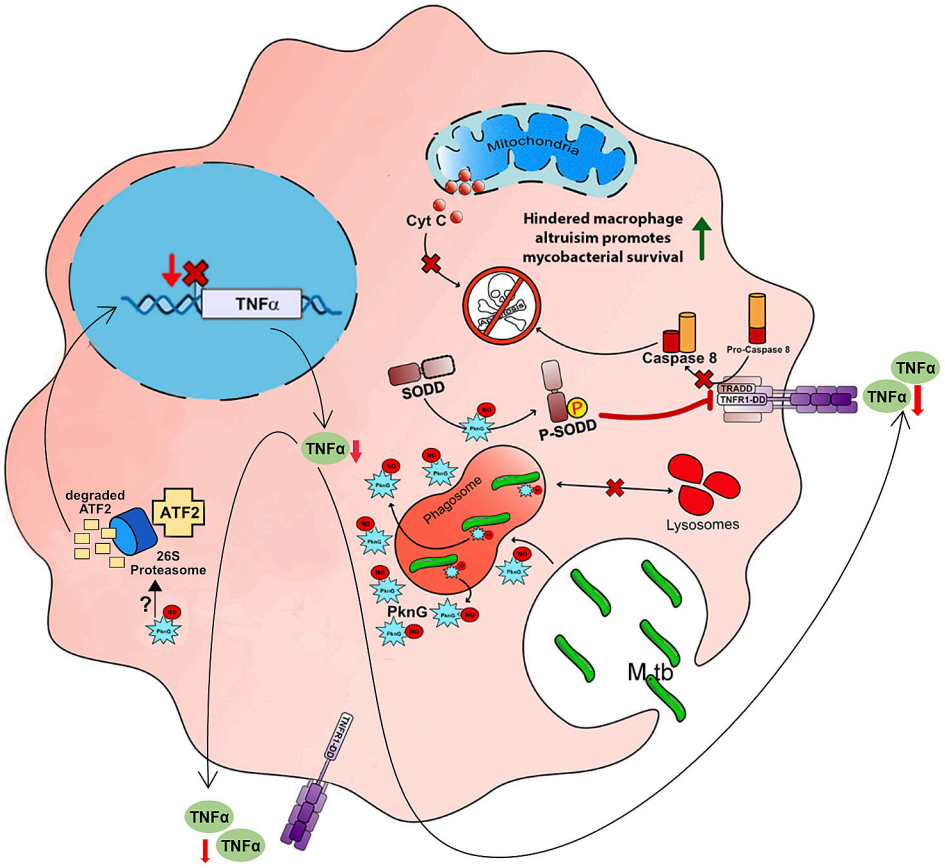

Fig. 6. Schematic representation of mycobacteria -secreted S-nitrosylated PknG-induced SODD phosphorylation and its consequent irreversible interaction with TNFR1 to prevent DISC formation and concomitant Caspase8 activation, which thereby prevents macrophage apoptosis and facilitates mycobacterial survival and proliferation. Simultaneously, S-nitrosylated PknG induces the degradation of ATF2, resulting in decreased TNFα production and thereby limiting apoptotic trigger in mycobacteria-infected macrophages.

Wild-type and mutant PknG complemented RvΔPG strains exhibited similar growth rates, membrane lipid composition (PDIM levels), and equivalent pathogenicity. Upon mycobacterial infection, PknG was secreted by Rv-, RvΔPG::PG-, and RvΔPG::PG^{K181M}-infected cells, thereby indicating the importance of S-nitrosylation of C109 of PknG for its secretion. Furthermore, AX17 and 4DMAA pretreated cells did not enable mycobacterial survival inside macrophages, nor did the kinase-dead or the S-nitrosylation-deficient PknG mutant expressing mycobacteria-infected cells, owing to significant levels of TNFα secretion and concomitant Caspase8 activation. Consequent to Caspase8 activation, loss of MMP, Caspase3 activation, and induction of apoptosis were observed in the S-nitrosylation-deficient or kinase-dead PknG-expressing mycobacteria-infected macrophages. Therefore, it was evident that mycobacterial infection results in S-nitrosylation of PknG on Cys109, facilitating its secretion and concomitant phosphorylation of SODD to prevent Caspase8 activation and apoptotic induction.

We next observed that in Rv-infected macrophages, phosphorylated SODD could compete with TRADD to bind irreversibly with TNFR1 death domain. While in RvΔPG-infected macrophages, in the absence of phosphorylated SODD, a TRADD–TNFR1 interaction induced DISC formation and concomitant Caspase8 activation. Moreover, CRISPR/Cas9-generated SODD knockout macrophages when expressing phosphomimetic SODD^{T405E} and not phosphoinert SODD^{T405A} could hinder Caspase8 activation and subsequent apoptotic induction upon infection with PknG-knockout mycobacteria. Interestingly, TNFα, although dependent on PknG-mediated macrophage substrate phosphorylation, was independent of SODD phosphorylation. Hence, rapid proteasomal degradation of TNFα-specific transcription factor ATF2, as was observed in this study, could be dependent on another PknG phosphorylated macrophage substrate. Besides, M.tb is known to form a separate TNFα-specific enhanceosome inside infected macrophages (38) which induces TNFα expression, plausibly at the late stages of infection, to facilitate programmed necrosis-mediated dissemination of proliferated mycobacteria (15). Therefore, it can be concluded that M.tb infection–triggered S-nitrosylation of PknG facilitates its secretion and concomitant phosphorylation of SODD to enable its irreversible interaction with TNFR1, to prevent DISC formation, Caspase8 activation, and thereby extrinsic apoptosis of infected macrophages.

The plethora of events orchestrated through S-nitrosylated PknG phosphorylated SODD was further established in vivo through our mice infection experiments. Rv, and PG expressing RvΔPG infected mice-obtained AVMΦ (isolated from BAL) exhibited SODD phosphorylation, which then interacts with TNFR1 and prevents DISC formation and Caspase8 activation. On the contrary, PknG knockout mycobacteria alone or when expressing kinase-dead or S-nitrosylation mutant of PknG were used to infect mice, the AVMΦ exhibited, activated Caspase 8, and Caspase3 leading to increased phosphatidylserine externalization, loss of MMP, formation of MOMP and DNA fragmentation, all indicative of apoptosis. It is intriguing as to why, RvΔPG-infected mice obtained AVMΦ, despite its ability to eliminate the pathogen, yet exhibit apoptotic or altruistic characteristics. Considering the labile nature of macrophages and owing to the complexity of its signaling network, it could well be that the infected AVMΦ of RvΔPG-infected mice exhibits altruism until the elimination of the internalized M.tb and thereafter triggers anastasis to regain its naïve form. Live tracking of such RvΔPG-infected AVMΦ inside mice can help resolve this puzzle.

Our work exhibits how successful pathogens like mycobacteria trick macrophages and utilize the initial proinflammatory trigger to dampen proinflammatory cytokine expression, secretion, and subsequent intracellular signaling, thereby facilitating its survival and proliferation at an early stage of infection. Moreover, S-nitrosylation triggered secretion of a virulent kinase, and subsequent facilitation of host substrate phosphorylation is innovative. The notion of secreted S-nitrosylated PknG-phosphorylated macrophage substrate to prevent macrophage apoptosis and thereby facilitate mycobacterial pathogenesis is established. "Dying to live" is an exit strategy inherent to macrophages, wherein their inability to curtail pathogenesis triggers their altruistic behavior to eliminate the pathogen along with itself (39). M.tb, in addition to its plethora of immune subversion mechanisms, utilizes the initial proinflammatory trigger-generated RNI to S-nitrosylate the Ser/Thr kinase PknG within itself, which thereby acts as the necessary secretory impetus. The S-nitrosylated PknG, once secreted inside macrophages, results in the phosphorylation of SODD, which then, by preventing Caspase8 activation, curbs the altruistic instincts of infected macrophages at the early stages of infection, thereby enabling mycobacteria to survive, establish its niche, and successfully proliferate within the macrophage. This phenomenon of hindered macrophage altruism makes mycobacteria a successful pathogen over ages and, owing to the rising drug-resistance menace, also provides us alternative opportunities for host-directed therapeutics against tuberculosis.

Materials and Methods

TMT-Switch Assay. The TMT-switch assay (40) was performed using the Pierce™ S-Nitrosylation Western Blot Kit. THP-1 cells expressing wild-type and Cys mutants of PknG were infected with RvΔPG, lysed, and immunoprecipitated with anti-PknG for one part, while the rest immunoblotted with anti-P-SODD and SODD. For the immunoprecipitated fractions, unmodified cysteines on proteins were blocked while S-nitrosylated cysteines were reduced with ascorbate. The TMT modified proteins were next detected using an anti-TMT.

Immunoblot Analysis. Purified recombinant proteins or total cell lysates of differentially treated or untreated and uninfected or different mycobacteria-infected macrophages (MOI 1:10) were lysed using RIPA buffer (Sigma) containing protease and phosphatase inhibitor cocktail (Roche) on ice for 20 min, followed by centrifugation at 16,000 g for 15 min at 4 °C. Lysates or immunoprecipitated samples were electrophoresed in 10% SDS-PAGE, transferred to PVDF (Merk Millipore) membrane, blocked, and thereafter probed with different primary and secondary antibodies, and finally developed using Supersignal WestPico (Thermo) substrate followed by visualization in LAS500 (GE).

Immunoprecipitation. Differentially treated or untreated macrophages were either uninfected or infected with different M.tb and thereafter lysed with IP-lysis buffer pH 8.0. Precleared lysates were incubated with specific antibody crosslinked Protein A/G agarose beads (39) and incubated in the same buffer at 4 °C for 2 h to overnight as required with slow rotation. The beads were washed thrice using lysis buffer and eluted using 100 mM glycine pH 5.3 for 10 min followed by neutralization using 1/10th volume of 1 M Tris pH8.0 and thereafter electrophoresed in 10% SDS-PAGE, transferred to PVDF membrane, and immunoblotted using indicated antibodies.

Estimation of Caspase3 and Caspase8 Activation. Caspase3 and Caspase8 activation, in uninfected, differentially treated, and mycobacteria-infected macrophages, were measured using FAM-DEVD-FMK and FAM-LETD-FMK (ImmunoChemistry Technologies), respectively, with fluorescence emission measured at 535 nm in a Cytation5 multimode reader (Biotek). Staurosporine (1 μM) treatment for 8 h or cyclohexamide treatment (10 μg/ml for 16 h) followed by human TNFα treatment (20 ng/ml for 4 h) was used as a positive control for inducing Caspase8 cleavage. Caspase8 activation in the experimental samples was measured after normalizing the obtained values with that of the staurosporine-induced cells, which were considered 100% Caspase8 activation.

CFU Assay of Mycobacteria-Infected THP-1 Cell Line and Mice. THP-1 cells, incubated with different M.tb strains for 90 min, were washed with RPMI1640 media containing amikacin, allowed to grow for 48 h, and thereafter washed with

PBS, lysed in 50 mM NaOH and 0.05% SDS-containing buffer and finally plated on Middlebrook 7H11 agar plates supplemented with cycloheximide (100 μg/ml). After three weeks of incubation at 37 °C, the obtained were counted as colony-forming units (CFU).

For mice experiments, first viable M.tb was determined by plating onto 7H11 agar plates containing 10% v/v OADC and incubation at 37 °C for 3 wk. These bacterial cultures were used to infect the mice using an aerosol chamber (Glas-Col). BALB/c mice aged 4 to 6 wk were either infected with aerosolized Rv or RvΔPG, RvΔPG::PG, RvΔPG::PG^{K181M}, and RvΔPG::PG^{C109G} (5×10^7 M.tb) or kept uninfected. After 24 h postinfection, one group of differently infected mice was sacrificed, and their lungs were isolated, homogenized in PBS at 4 °C followed by plating of the homogenate in 7H11 agar plates, and incubated at 37 °C. CFU counts were taken after 21 d of incubation. For another set of similarly infected mice, infection was allowed to proceed for 48 h, after which BAL was separately obtained from these mice, and AVMΦ was isolated as indicated. Isolated AVMΦ was processed for immunofluorescence and TUNEL assay. For the third set of similarly infected mice, the infection was allowed to continue for 21 d; thereafter, the mice were sacrificed, and their lungs were isolated and processed for plating.

Immunofluorescence. Isolated AVMΦs were fixed with 4% paraformaldehyde for 15 min, permeabilized with 0.02% saponin for 10 min, blocked using 5% FBS for 1 h, and thereafter incubated with desired primary antibody diluted in blocking buffer for 2 h to 8 h at 4 °C followed by 3 to 4 washes using TBS-T and Alexa Fluor488/568/647–conjugated anti-isotypic secondary antibody incubation for 1 h. Next, after counterstaining with DRAQ5, slides were mounted onto coverslips using ProLong AntiFade Gold and imaged under an Olympus FV3000 laser scanning confocal microscope.

Data, Materials, and Software Availability. All study data are included in the article and/or *SI Appendix*.

ACKNOWLEDGMENTS. We thank ICMR-NIJOLMD and ICMR-NIRT Chennai for providing access to BSL3 facility. Special thanks go to technicians of ABSL3 facility at ICMR-NIJOLMD for mice infection studies; Prof. Yousef Av-Gay, University of British Columbia, and Prof. Vinay Nandicoori from NII, Delhi, for providing Rv and RvΔPknG mycobacteria; and Prof. Jean Pieters for kindly providing PknG, $PknG^{K181M}$ constructs and for valuable suggestions. SS, SR, AH, and DD are thankful to MoE, GoI, and IIT Kharagpur for providing fellowship, infrastructural, and instrumentation facilities. SBD is thankful to IIT Kharagpur and DBT Ramalingaswami Re-entry fellowship (BT/RLF/Re-entry/33/2014), DBT-IDB (BT/PR26821/MED/30/1938/2017-reg), DST-SERB (CRG/2020/000748), DST-FIST Phase II (F. No.: 3-18/2015-TS-TS.I), and ICMR (2021-8995/CMB/ADHOC-BMS) for their financial support.

Author affiliations: [a]Molecular Immunology and Cellular Microbiology Laboratory, Department of Bioscience and Biotechnology, Indian Institute of Technology Kharagpur, Kharagpur 721302, India; [b]Laboratory for Animal Experiments, ICMR-National JALMA Institute for Leprosy and Other Mycobacterial Diseases, Agra 282006, India; [c]Department of Microbiology and Molecular Biology, Indian Council of Medical Research (ICMR)-National Japanese Leprosy Mission for Asia (JALMA) Institute for Leprosy and Other Mycobacterial Diseases, Agra 282006, India; [d]Department of Bacteriology, National Institute for Research in Tuberculosis, Chennai, Tamil Nadu 600031, India; and [e]ICMR—National Institute for Research in Environmental Health, Bhopal 462030, India

Author contributions: S.B.D. conceptualized research; S.B.D. designed research; S.B.D., S.S., S.R., A.H., and D.D. performed research; V.K., A.K.S., A.V.S., and R.M. designed experiments; A.V.S. and R.M. provided access to BSL3 facility at NJILOMD and NIRT; S.S., S.R., A.H., and S.B.D. analyzed data; V.K. and A.K.S. provided access to ABSL3 facility at NJILOMD; and S.B.D., S.S., S.R., and A.H. wrote the paper.

1. World Health Organization, "Global tuberculosis report 2022". https://iris.who.int/handle/10665/363752. License: CC BY-NC-SA 3.0 IGO. Deposited 27 October, 2022.
2. D. T. Anley *et al.*, Prognostication of treatment non-compliance among patients with multidrug-resistant tuberculosis in the course of their follow-up: A logistic regression-based machine learning algorithm. *Front Digit Health.* **5**, 1165222 (2023).
3. S. Gagneux, Ecology and evolution of Mycobacterium tuberculosis. *Nat. Rev. Microbiol.* **16**, 202–213 (2018).
4. S. Saha *et al.*, A bumpy ride of mycobacterial phagosome maturation: Roleplay of coronin1 through cofilin1 and camp. *Front. Immunol.* **12**, 687044 (2021).
5. S. Bosedasgupta, J. Pieters, Inflammatory stimuli reprogram macrophage phagocytosis to macropinocytosis for the rapid elimination of pathogens. *PLoS Pathog.* **10**, e1003879 (2014).
6. S. Saha, P. Das, S. BoseDasgupta, "It takes two to tango": Role of neglected macrophage manipulators coronin 1 and protein kinase g in mycobacterial pathogenesis. *Front. Cell Infect. Microbiol.* **10**, 582563 (2020).
7. S. M. Behar, V. Briken, Apoptosis inhibition by intracellular bacteria and its consequence on host immunity. *Curr. Opin. Immunol.* **60**, 103–110 (2019).
8. S. M. Behar *et al.*, Apoptosis is an innate defense function of macrophages against Mycobacterium tuberculosis. *Mucosal. Immunol.* **4**, 279–287 (2011).
9. S. M. Behar, M. Divangahi, H. G. Remold, Evasion of innate immunity by Mycobacterium tuberculosis: Is death an exit strategy? *Nat. Rev Microbiol.* **8**, 668–674 (2010).
10. T. H. Mogensen, Pathogen recognition and inflammatory signaling in innate immune defenses. *Clin. Microbiol. Rev.* **2**, 240–73 (2009).
11. P. Chandra, S. J. Grigsby, J. A. Philips, Immune evasion and provocation by Mycobacterium tuberculosis. *Nat. Rev. Microbiol.* **20**, 750–766 (2022).
12. A. M. Cooper, K. D. Mayer-Barber, A. Sher, Role of innate cytokines in mycobacterial infection. *Mucosal. Immunol.* **4**, 252–260 (2011).
13. L. B. Adams, M. C. Dinauer, D. E. Morgenstern, J. L. Krahenbuhl, Comparison of the roles of reactive oxygen and nitrogen intermediates in the host response to Mycobacterium tuberculosis using transgenic mice. *Tuber Lung Dis.* **78**, 237–46 (1997).
14. B. Carow *et al.*, Silencing suppressor of cytokine signaling-1 (SOCS1) in macrophages improves Mycobacterium tuberculosis control in an interferon-gamma (IFN-gamma)-dependent manner. *J. Biol. Chem.* **286**, 26873–87 (2011).
15. F. J. Roca, L. J. Whitworth, S. Redmond, A. A. Jones, L. Ramakrishnan, TNF induces pathogenic programmed macrophage necrosis in tuberculosis through a mitochondrial-lysosomal-endoplasmic reticulum circuit. *Cell.* **178**, 344–1361.e11 (2019).
16. D. R. Roach *et al.*, TNF regulates chemokine induction essential for cell recruitment, granuloma formation, and clearance of mycobacterial infection. *J. Immunol.* **168**, 4620–4627 (2002).
17. M. S. Hayden, S. Ghosh, Regulation of NF-κB by TNF family cytokines. *Semin. Immunol.* **26**, 253–266 (2014).
18. G. van Loo, M. J. M. Bertrand, Death by TNF: a road to inflammation. *Nat. Rev. Immunol.* **23**, 289–303 (2023).
19. M. Yuk, J. K. Kim, I. S. Kim, E. K. Jo, TNF in human tuberculosis: A double-edged sword. *Imune Netw.* **24**, e4 (2024).
20. M. M. Rahman, G. McFadden, Modulation of tumor necrosis factor by microbial pathogens. *PLoS. Pathog.* **2**, e4 (2006).
21. Z. Hmama, S. Peña-Díaz, S. Joseph, Y. Av-Gay, Immunoevasion and immunosuppression of the macrophage by Mycobacterium tuberculosis. *Immunol. Rev.* **264**, 220–232 (2015).
22. A. Koul, T. Herget, B. Klebl, A. Ullrich, Interplay between mycobacteria and host signalling pathways. *Nat. Rev. Microbiol.* **2**, 189–202 (2004).
23. A. Walburger *et al.*, Protein kinase G from pathogenic mycobacteria promotes survival within macrophages. *Science.* **304**, 1800–1804 (2004).
24. N. Scherr *et al.*, Survival of pathogenic mycobacteria in macrophages is mediated through autophosphorylation of protein kinase G. *J. Bacteriol.* **191**, 4546–4554 (2009).
25. S. B. Dasgupta, J. Pieters, Striking the right balance determines TB or Not TB. *Front. Immunol.* **5**, 455 (2014).
26. B. Rieck *et al.*, PknG senses amino acid availability to control metabolism and virulence of Mycobacterium tuberculosis. *PLoS. Pathog.* **13**, e1006399 (2017).
27. D. W. Banner *et al.*, Crystal structure of the soluble human 55 kd TNF receptor-human TNF beta complex: Implications for TNF receptor activation. *Cell.* **73**, 431–445 (1993).
28. H. Hsu, H. B. Shu, M. G. Pan, D. V. Goeddel, TRADD-TRAF2 and TRADD-FADD interactions define two distinct TNF receptor 1 signal transduction pathways. *Cell.* **84**, 299–308 (1996).
29. Y. Jiang, J. D. Woronicz, W. Liu, D. V. Goeddel, Prevention of constitutive TNF receptor 1 signaling by silencer of death domains. *Science.* **283**, 543–546 (1999).
30. F. J. Roca, L. J. Whitworth, H. A. Prag, M. P. Murphy, L. Ramakrishnan, Tumor necrosis factor induces pathogenic mitochondrial ROS in tuberculosis through reverse electron transport. *Science.* **376**, eabh2841 (2022).
31. A. Ashkenazi, V. M. Dixit, Death receptors: Signalling and modulation. *Science.* **281**, 1305–1308 (1998).
32. M. Wittwer, Q. Luo, V. R. Kaila, S. A. Dames, Oxidative unfolding of the rubredoxin domain and the natively disordered N-terminal region regulate the catalytic activity of mycobacterium tuberculosis protein kinase g. *J. Biol. Chem.* **291**, 27062–27072 (2016).
33. A. Martínez-Ruiz, S. Lamas, S-nitrosylation: A potential new paradigm in signal transduction. *Cardiovasc Res.* **62**, 43–52 (2004).
34. N. O. Devarie-Baez, D. Zhang, S. Li, A. R. Whorton, M. Xian, Direct methods for detection of protein S-nitrosylation. *Methods.* **62**, 171–176 (2013).
35. L. Cerveny *et al.*, Tetratricopeptide repeat motifs in the world of bacterial pathogens: Role in virulence mechanisms. *Infect Immun.* **81**, 629–35 (2013).
36. M. Gil *et al.*, New substrates and interactors of the mycobacterial Serine/Threonine protein kinase PknG identified by a tailored interactomic approach. *J. Proteomics.* **192**, 321–333 (2019).
37. M. W. Foster, D. T. Hess, J. S. Stamler, Protein S-nitrosylation in health and disease: A current perspective. *Trends Mol. Med.* **15**, 391–404 (2009).
38. R. Barthel *et al.*, Regulation of tumor necrosis factor alpha gene expression by mycobacteria involves the assembly of a unique enhanceosome dependent on the coactivator proteins CBP/p300. *Mol. Cell. Biol.* **23**, 526–533 (2003).
39. M. Divangahi, S. M. Behar, H. Remold, Dying to live: How the death modality of the infected macrophage affects immunity to tuberculosis. *Adv. Exp. Med. Biol.* **783**, 103–120 (2013).
40. C. I. Murray, H. Uhrigshardt, R. N. O'Meally, R. N. Cole, J. E. Van Eyk, Identification and quantification of S-nitrosylation by cysteine reactive tandem mass tag switch assay. *Mol Cell Proteomics.* **11**, M111.013441 (2012).